THE MUON COLLIDER—STATUS AND PHYSICS PROSPECTS[1]

RAJENDRAN RAJA

Fermilab,P.O.Box 500, Batavia, Il 60510, USA,

E-mail:raja@fnal.gov

The current status of the muon collider is presented, with a brief historical review. The proton source and the pion production and decay channel needed for a first muon collider (FMC) are described. A brief review of ionization cooling theory is followed by the cuurent status of cooling ideas. The acceleration scheme and the collider ring are presented, followed by the backgrounds expected in a muon collider detector and the physics potential of such a detector. The physics potential of a muon storage ring that acts as an intense neutrino source of well-defined flavor is reviewed.

1 Brief Historical Overview

To collide muons is not a new idea. Muon storage rings were mentioned by Tinlot and Green [1] as early as 1965, and further investigated by Budker[2] in 1969 and Skrinsky[3] in 1971 and Neuffer[4] in 1979. The key concept of ionization cooling was described by Skrinsky and Parkhomchuk[6] in 1981. The realization that a high luminosity muon collider might be feasible[5] resulted in a series of workshops. After the Sausalito workshop in 1995, Fermilab and Brookhaven joined in an effort to study the concept and publish a report. The muon collider collaboration has grown to twenty-six institutions and approximately a hundred physicists. A feasibility study at Snowmass, Colorado in 1996 resulted in the study of a 2 x 2 TeV collider. The muon collider collaboration has continued to develop the concepts. The Fermilab workshop[7] on physics at the first muon collider and the front end of the muon collider in 1997 brought together schemes to utilize the full potential of the muon collider complex. The status of current research in this field can be obtained from a lengthy article[8] published in PRSTAB.

[1] Invited talk presented at the Worldwide Study on Physics and Experiments with Future Linear e^+ e- colliders, Sitges (Barcelona), Spain, April 1999.

2 Motivation

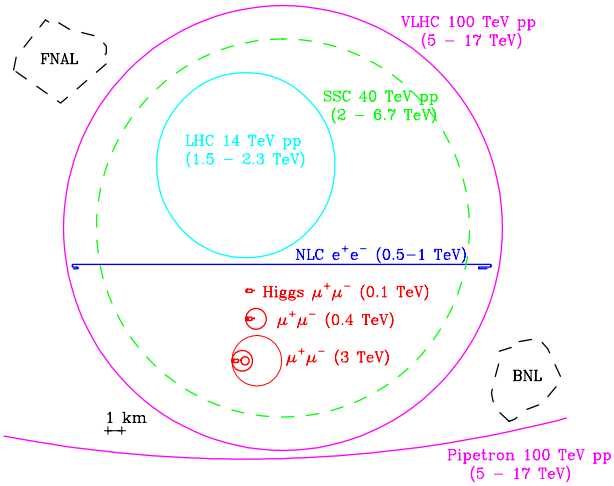

Figure 1 Comparison of the sizes of various machines vs existing laboratory sites.

The mass of the muon is 200 times larger than that of the electron. This permits the construction of compact machines that fit on existing laboratory sites. Figure 1 compares the sizes of various proposed accelerators to existing laboratory sites at Brookhaven and Fermilab. The cross section for producing the Higgs boson directly in the s-channel is ~40,000 that of the electron case, as a result of the larger muon mass. Thus Higgs bosons and Higgs-like techni-entities such as the techni –rho and the techni-eta can be produced in the s-channel in a muon collider.

The energy spread of the beam in a muon collider is much smaller than the electron case, since both beamsstrahlung and initial state radiation effects are much smaller. Such small energy spreads would permit the scanning of narrow resonances such as a light standard model Higgs boson (mass 120 GeV/c^2 and width 2-3 MeV/c^2). The energy of the muon beam can be determined to a precision of 10^{-6} using g-2 precession of the muon[9].

Muons of both charges can be polarized. Polarizations of ~25% are easy to achieve and can be utilized to good advantage. Higher polarizations are reachable by making tighter selections on the accepted phase space during muon capture. Another important motivation is the ability of the muon collider to reach higher energies, once the problems associated with a relatively low energy machine are solved. Also, as a muon collider is being built, the intense proton source needed can be used for collider physics and rare K physics and the cold muons available can be utilized for a variety of muon experiments such as $\mu \rightarrow e\gamma$.

One of the main conclusions of the Fermilab Workshop [7] was that muon storage rings offer a unique means to produce intense neutrino beams of known flavor content and kinematics. Such beams can be used to enhance our knowledge

of neutrino oscillation physics significantly and may be a first step towards a muon collider.

3 Overall Scheme

Protons from an intense proton source (1.5 x 10^{22} protons/year) in 1ns bunches are used to produce pions. The muons resulting from the pion decay are collected and bunched together. The 6 dimensional phase space of the decay muons has to be reduced by a factor of ~10^6 before the muons can be accelerated and made to collide. This cooling of the phase space is achieved by subjecting the muon bunches to energy loss by ionization while maintaining their longitudinal momentum by rf power. Figure 2 shows a schematic of a muon collider complex from beginning to end.

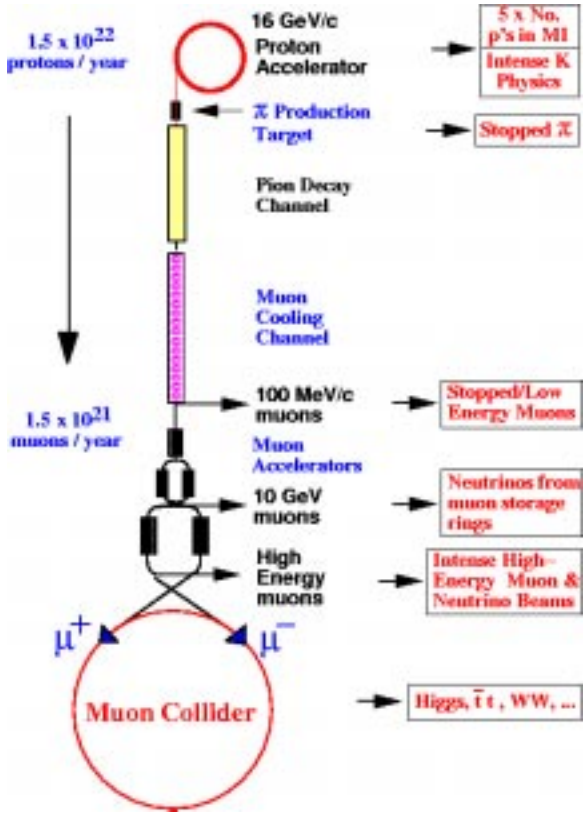

Figure 2 Schematic of a muon collider

Three collider center of mass energies have been investigated in some detail to date, 0.1 TeV, 0.4 TeV and 3 TeV. The first is the so-called Higgs Factory and has two momentum spread options, the narrow-band option being used to scan the Higgs resonance in the s-channel. The 0.4 TeV option will permit one to operate above the top quark threshold and the 3 TeV option will push the energy range of the searches to beyond the LHC regime. Table 1 shows the parameters associated with each option.

Table 1 Muon Collider parameters.

	Center of mass Energy (GeV)			
	100		400	3000
	Broadband	Narrowband		
Rate(Hz)	15	15	15	15
Muons/bunch	$4x10^{12}$	$4x10^{12}$	$2x10^{12}$	$2x10^{12}$
Bunches	1x1	1x1	2x2	2x2
Circumference	300m	200m	1km	6km
Bunch σ_z(cm)	9	13	2.3	0.3
Spot σ_r(μm)	187	270	24	3.2
β*(cm)	9	13	2.3	0.3
ΔE/E(%)	0.007	0.002	0.08	0.08
L(cm^{-2} s^{-1})	$2x10^{31}$	$1x10^{31}$	10^{33}	$5x10^{34}$

We will now describe each of the component systems that make up the muon collider in some detail.

4 The proton Source

The muon production rate is not very sensitive to the choice of proton driver energy since the increased pion poduction rate at higher energy is compensated by the higher repetition rate at lower energy. The challenge is to produce very short (~1ns) intense (~10^{13} protons/bunch) proton bunches at a repetition rate of 15 Hz. A particular scheme to upgrade the Fermilab proton source has been discussed [10] that upgrades the Linac energy from 400 MeV to 1 GeV and the booster energy from 8 GeV to 16 GeV. There are also plans to add a 3 GeV pre-booster that facilitates short bunches. A design sudy is currently in progress.

5 Pion Collection and decay

The intense proton bunches are targeted on to a liquid metal target (the current favorite is mercury) that sits in a 20 Tesla solenoid. This corresponds to an average beam power of 4 megawatts. Pions with p_T < 200 MeV/c are captured in this

solenoid. They are then transferred to solenoids of 1.25 Tesla field that house rf cavities that help to bunch the pions and the decay muons. This solenoid decay channel is also referred to as the phase rotation channel, in accelerator jargon. Current simulations call for $2x10^{22}$ protons per year on target. The pion capture channel accepts 0.6 π's per proton with an average p_z, p_T of ~ 200 MeV/c. The fractional beam energy spread is ~ 100%. This scheme is illustrated in Figure 3. One of the main challenges here is to handle the 400 Kilowatts of power deposited on target.

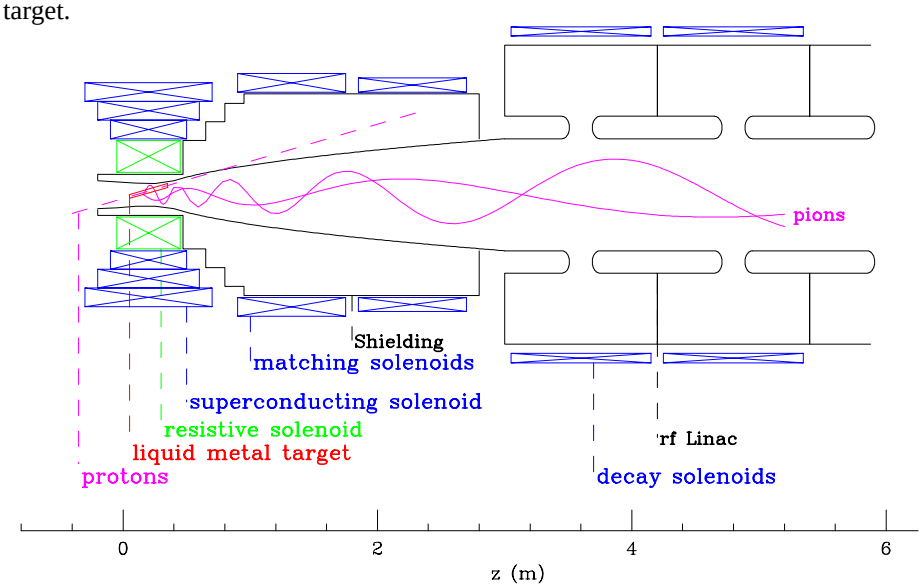

Figure 3 Schematic pion capture and decay system

The first rf cavity of the phase rotation channel is ~3m downstream of the target. One of the unknowns is how well the cavity will perform in the presence of the intense radiation. An experiment has been approved at Brookhaven to test these ideas[11].

6 Ionization Cooling

In a Hamiltonian system, a particle's motion along the beam direction may be specified by a set of 6 canonical variables $(x,p_x),(y,p_y)$,(z,p_z) or $(x,p_x),(y,p_y),(E,t)$, where x,y,z denote the co-ordinates with z the beam direction and p_x,p_y,p_z, denote the momentum components and E,t denote the energy and time of the particle. Let X_i (i=1,6) denote the 6 vector set. Then the error matrix E over an ensemble of particles (otherwise known as beam) is defined by $E_{ij} = \langle X_iX_j\rangle - \langle X_i\rangle\langle X_j\rangle$, the <> denoting average over the ensemble of particles. The 6 dimensional emittance ε_6 is

defined by $(\varepsilon_6)^2$ = determinant(E)/$(m_\mu c)^6$. In a Hamiltonian linear system the 6-vector X' at a later time is given by a linear transformation U such that $X' = UX$, leading to $E' = UEU^T$ .This implies that det(E') = det(E), i.e emittance is preserved if det(U) = 1. For Hamiltonian systems, it can be shown that det(U) =1. Such transformations are known as symplectic transformations. This result for Hamiltonian systems is an example of Liouville's theorem. Cooling a beam implies reducing its emittance which in turn implies transformations such that det(U)<1 and necessarily non-Hamiltonian systems.

Due to the short lifetime of the muon, stochastic cooling techniques are not feasible, as they are too slow. It is possible, however, to remove energy from the muons by ionization losses[6], since the muons have long interaction lengths with matter and do not produce electromagnetic showers frequently. The energy is lost by dE/dx in an absorber. The longitudinal component of the beam momentum is maintained by radio-frequency cavities resulting in a reduction of the transverse emittance of the beam.

The 6-D emittance ε_6 can be written as a product of transverse and longitudinal emittances in the case where longitudinal and transverse correlations can be neglected, i.e $\varepsilon_6 = (\varepsilon^x_n)\,(\varepsilon^y_n)\,(\varepsilon^z_n)$. In the limit where angles θ_i of the particles with the beam direction are small, one can write the normalized transverse emittance $(\varepsilon^x_n)^2 = \{<x^2><\theta^2>-<x\theta>^2\}\gamma^2\beta^2$. The term in {} is known as the unnormalized emittance and $\gamma\beta$ are the usual Lorentz factors of the beam. Differentiating the expression for ε^x_n with respect to z, leads to the following expressions.

$$\frac{d\varepsilon_N^x}{dz} = \varepsilon^x \frac{d(\beta\gamma)}{dz} + \beta\gamma \frac{d\varepsilon^x}{dz}$$

The first term is the cooling term and the second the heating term. The cooling term can be re-written $\frac{d\varepsilon_N^x}{dz}(cool) = -\frac{1}{\beta^2}\frac{\varepsilon_N^x}{E}\left|\frac{dE}{dz}\right|$ and the heating term as

$$\frac{d\varepsilon_N^x}{dz}(heat) = \frac{\beta\gamma}{2\varepsilon_x}\left\{<x^2>\frac{d<\theta^2>}{dz} + <\theta^2>\frac{d<x^2>}{dz} - 2<x\theta>\frac{d<x\theta>}{dz}\right\}$$

Neglecting correlations between x and θ, this can be re-written as

$$\frac{d\varepsilon_N^x}{dz}(heat) = \beta\gamma\frac{\beta_\perp}{2}\frac{d<\theta^2>}{dz}$$

The last term describes the increase in angular divergence as a result of multiple scattering, which leads finally to

$$\frac{d\varepsilon_N^x}{dz} = -\frac{1}{\beta^2}\frac{\varepsilon_N^x}{E}\left|\frac{dE}{dz}\right| + \frac{\beta_\perp}{2\beta^3 E m_\mu L_R}(0.014)^2$$, where $\beta_\perp$ is the beta function from focusing theory, L_R is the radiation length of the absorber and m_μ the mass of the muon.

The last equation shows the rate of change of emittance as a function of z. The first term depicts cooling due to ionization and the second term depicts heating due to multiple scattering. This heating is smaller, the smaller the beta function of the lattice. This is because at these focusing points, the angular divergence of the beam is large and the additional noise from multiple scattering has the least effect. It can be seen that the rate of cooling is proportional to the emittance, i.e, the cooler the beam, the harder it is to cool. This is an example of the third law of thermodynamics. There is also an equilibrium minimum emittance at which the heating and the cooling terms balance. In order to reach lower equilibrium emittances, one needs stronger focusing and low atomic number absorbers with large radiation lengths. The Muon Collider collaboration currently favors the scheme shown in Figure 4 for cooling. It has so far received the most study.

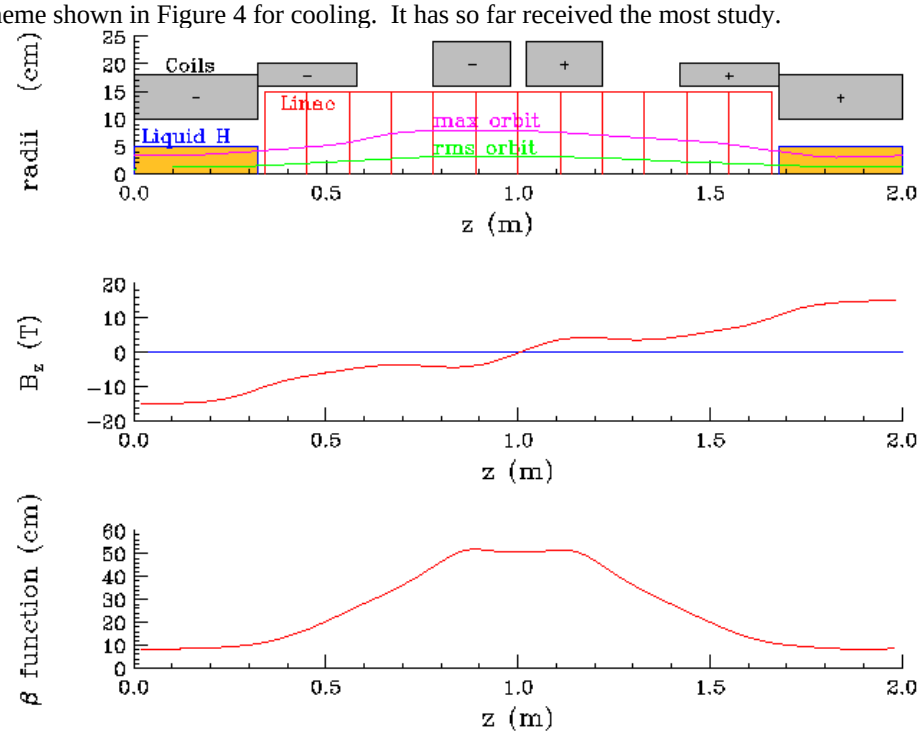

Figure 4 Top plot shows one cell of the alternating solenoid scheme, with the liquid hydrogen absorber and the rf module. The middle plot shows the variation of the magnetic field and the bottom plot, the beta function vs distance.

Solenoids with magnetic field alternating in direction are used to contain and transport the muon beam. The fields in neighboring solenoids alternate so as to control the angular momentum of the beam. The absorber made of liquid hydrogen is placed at the low beta points in the middle of the solenoids. The rf module straddles solenoids and maintains the longitudinal momentum of the beam. Such a scheme can be used to cool the beam till the emittance becomes comparable to the equilibrium emittance. At this point liquid lithium lenses are contemplated to take over and focus the beam further as well as act as absorbers.

6.1 Longitudinal emittance exchange

The spread of the beam in the longitudinal direction increases as the cooling proceeds because of straggling. The non-zero value of the mean longitudinal momentum leads to this asymmetric behavior between longitudinal and transverse cooling. The method currently under consideration to reduce the longitudinal emittance is to bend the particles and pass them through a wedge-shaped absorber such that the faster particles pass through more material. It can be shown that this results in a decrease in the longitudinal emittance and an increase in the transverse emittance. The increased transverse emittance is further reduced in the following transverse cooling sections. Figure 5 shows a scheme for longitudinal emittance exchange that is currently under study. Bent solenoids are used to induce dispersion in the beam and the wedge-shaped absorbers are placed at points where the beam is dispersed. The bending occurs in x and y directions using double-bent solenoids to preserve x-y symmetry.

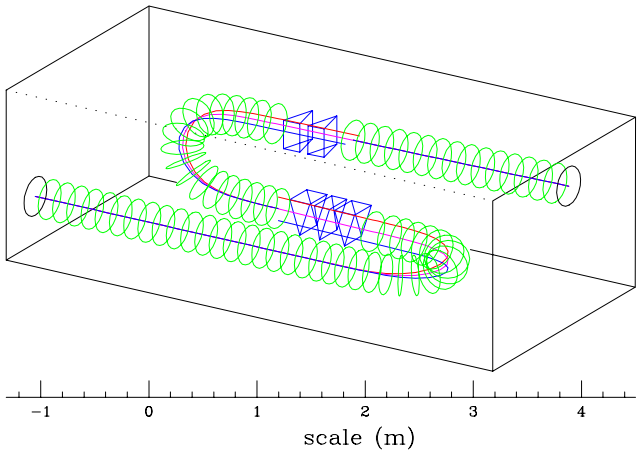

Figure 5 Double-bent solenoid longitudinal emittance exchange scheme.

Figure 6 shows the decrease in transverse and longitudinal emittance as the cooling proceeds through a cooling system consisting of alternating solenoids, emittance exchange sections and lithium lenses. The longitudinal emittance increases in the lithium lenses, but is more than adequately compensated by the decreases in transverse emittances. A total cooling factor of ~10^6 is currently called before the muon beam can be accelerated. There exist several remaining problems in the cooling design, the main ones being that of matching between the collection stage and the cooling section and the complete design of the emittance exchange section.

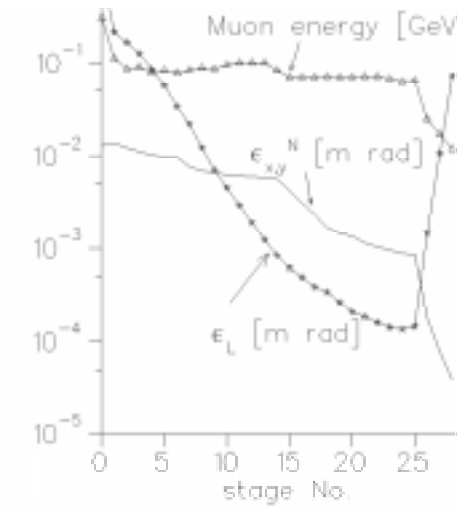

Figure 6 Average energy of the muon and transverse and longiduinal emittances as a function of the cooling stage. As the lithium lenses take over towards the end, longitudinal emittance increases and the average energy of the muons decreases.

7 Acceleration and collision

Acceleration of muons is currently being given a thorough study. Superconducting re-circulating linacs (RLA's) as employed at Jefferson National Laboratory (formerly CEBAF) look promising. Table 2 shows the results of a preliminary study of this option.

We have also studied collider lattices which have the correct low beta characteristics for the 0.1 TeV and 4 TeV center of mass energy case. The muons circulate for approximately 1000 turns before they decay by a factor 1/e.

Table 2 RLA parameters

	RLA1	RLA2	RLA3	RLA4
E(start) GeV	1.0	9.6	70	250
E(end)GeV	9.6	70	250	2000
No. turns	9	11	12	16
Arc length(m)	30	175	520	3500
Linac length (m)	100	300	533	2800
Gradient (MV/m)	5	10	15	20
Decay losses (%)	9.0	5.2	2.4	3.6

8 Physics at the First Muon Collider

8.1 Muon Polarization

Pions when they decay produce muons that are fully polarized individually. However, the muons are emitted isotropically in the pion rest frame, leading to a total zero polarization, if all the muons are accepted. One can increase the muon polarization by selecting muons that decay forward in the pion center of mass. Figure 7 shows the muon polarization vs F_{surv} , the fraction of muons accepted before and after cooling. It can be seen that polarization of 25% for each beam is easily achievable without too great a loss in intensity.

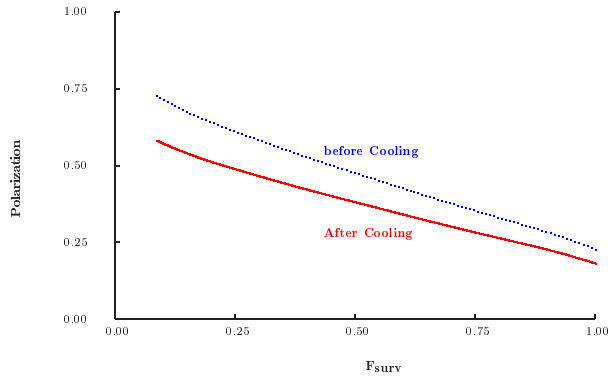

Figure 7 Polarization of muons before and after cooling as a function of the fraction accepted.

This polarization can be put to good use. It enables one to determine the energy of the muon bunches to a precision of a part in 10^6 using g-2 precession of the polarization[9]. If the machine energy is stable to a part in 10^5, the width of s-channel Higgs bosons (width/mass ~10^5) can be measured by scanning[12].

8.2 s –channel Higgs production.

As mentioned, the coupling of Higgs like particles to the $\mu\mu$ initial state is ~40,000 times greater than that of the corresponding *ee* initial state. This coupled with the narrow momentum spreads achievable in the muon collider and the precise energy calibration permits one to scan the Higgs resonance. Figure 8 shows the effective Higgs cross section as a function of the beam momentum resolution[12]. The narrower the beam spread, the greater the value of the central peak cross section.

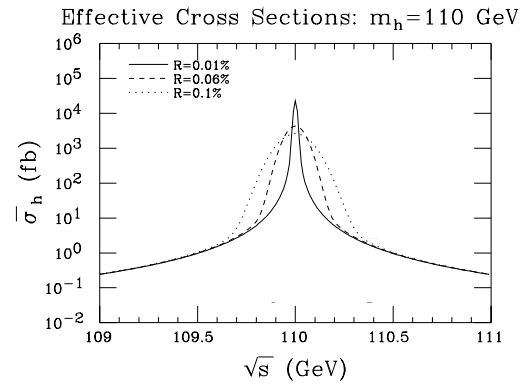

Figure 8 Effective Higgs cross-section for various beam momentum resolutions.

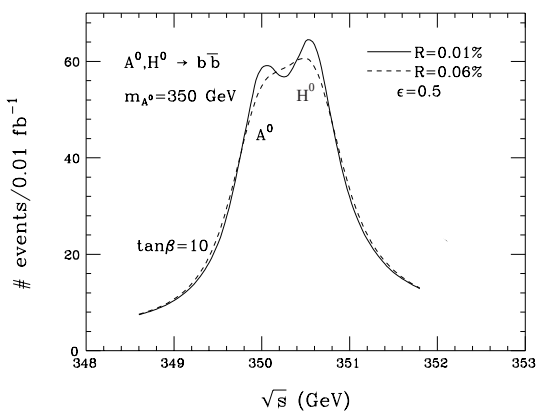

Figure 9 Separation of A^0 and H_0 signals for tan β=10

It is possible to measure the width[8] of the Higgs boson to 16%, σ.B(b $\bar{b}$) =1% and σ.B(WW*)=5% with an integrated luminosity of 0.4fb^{-1}. In the Minimal Supersymmetric extension of the standard model (MSSM), the width of the lowest mass Higgs boson h^0 is 2-3 MeV if tan β ~1.8 and 2-800 MeV if tan β ~20 for Higgs masses in the range 110-130 GeV/c^2. The ratio r of Higgs branching ratios to b $\bar{b}$ and WW* is sensitive to the A^0 mass for m_{A0} <500 GeV/c^2. The ratio r_{MSSM}/r_{SM} =0.3,0.5,0.8 for m_{A0}=200,250,400 GeV/c^2[12]. So it may be possible by scanning the Higgs at the muon collider not only to test if it is a standard model object but also to glean some information on the mass of A^0. In the decoupling limit of MSSM, the masses of H^0 and A^0 are almost degenerate. The fine resolution of the muon collider would then enable one to resolve the peaks as can be seen from

Figure 9. Technicolor objects that couple like the Higgs can also benefit from such an s-channel scan[13].

8.3 Threshold scans

The better momentum resolution of the muon collider again permits the scanning of the W and top thresholds as well as the numerous other thresholds expected in SUSY. The W mass can be determined to a precision of 20 MeV, the top quark mass to 200 MeV and the Higgs mass to 140 MeV by a scan of the Z h threshold.

8.4 Heavy SUSY scalar pair production

These thresholds are P-wave suppressed, so for scalar masses of ~ 1 TeV, center of mass energies of 3-4 TeV are needed to adequately measure the cross section[14]. The greater energy reaches feasible in a muon collider would be useful, should this be the SUSY scenario chosen by nature.

9 Detectors and backgrounds

The collaboration has done some preliminary work on backgrounds due to muon halo in the collider ring. Preliminary results suggest that a scraper system would be effective in reducing halo by a factor of 10^3. Backgrounds at the interaction region due to pair production of electrons have been studied. It is believed that these pairs can be confined to be near the beam pipe region by the use of a strong solenoidal magnetic field of strength ~4 Tesla.

The main backgrounds at the detector, however, come from the decay of the muons in the beam pipe and the resultant decay electron showers. These showers result in low energy (~1 MeV) photons, which interact with nuclei producing neutrons via the giant dipole resonance. These neutrons and the low energy photons are difficult to contain and cause knock-on proton and electron backgrounds in the detector. In addition to this, there is pair production of muons in the elctromagnetic shower. These Bethe-Heitler muons occur at the rate of a part in 10^4 in the shower process. The large number of muon decays however ensure that a sufficient number of these Bethe-Heitler muons will enter the detector volume to be of concern especially at primary muon beam energies of over 1 TeV.

Significant improvements have been made in shielding the detector against these backgrounds using sweeping magnets and well-designed tungsten cones that prevent backscattered shower fragments from entering the detector[8][15]. Figure 10 shows the occupancy as a function of radial distance from the interaction point and muon beam momentum for silicon pads of 300μmx300μm due to charged and neutral particles. Figure 11 shows the occupancy due to charged particles alone. Table 3 shows a detailed breakdown of the occupancy vs radial distance for the

Higgs factory. Based on these numbers, we calculate a silicon lifetime of 8 years for the Higgs factory and 5 years for the 4 TeV center of mass collider.

Table 3. Occupancy vs radius for the Higgs factory

Radius	***cm***	***5***	***10***	***20***	***100***
Photon hits	cm^{-2}	26	6.6	1.6	0.06
Neutron hits	cm^{-2}	0.06	0.08	0.2	0.04
Charged hits	cm^{-2}	8	1.2	0.2	0.01
Total hits	cm^{-2}	34	8	2	0.12
Pixel size	µm x µm	60 x 150	60 x 150	300x300	300 x 300
Total occupancy	%	0.6	0.14	0.4	0.02
Occupancy from Charged particles	%	0.14	0.02	0.04	0.002

Bethe-Heitler muons deposit energy in the calorimeter. Due to the large numbers that get through and the non-gaussian tail from catastrophic brehmsstrahlung, they can cause problems especially at the higher beam energies. We are currently investigating schemes to minimize their effects by calorimeter timing (1ns time resolution), since they are out of time with the particles from the interaction. For details, see the status report[8].

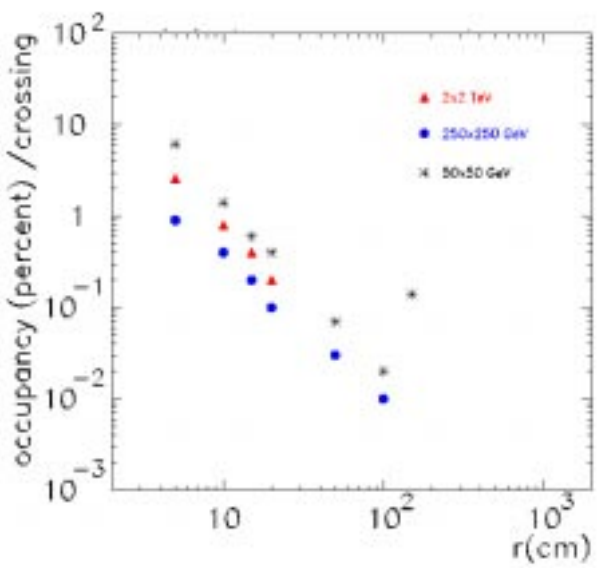

Figure 10 Total occupancy due to neutral and charged particles as a function of radius and muon beam energy

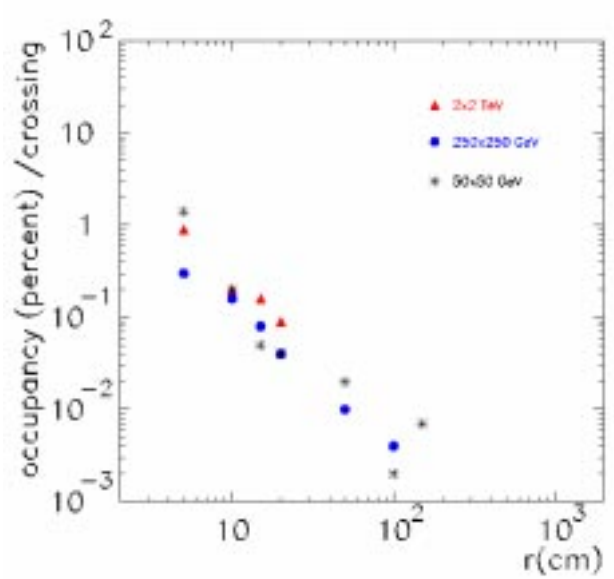

Figure 11 Occupancy due to charged particles as a function of radius and muon beam energy.

We have described a strawman detector in Geant and are investigating the problem of pattern recognition in the presence of these backgrounds. Figure 12 shows a cutaway Geant view of the detector. For details on the various detector options see the status report[8].

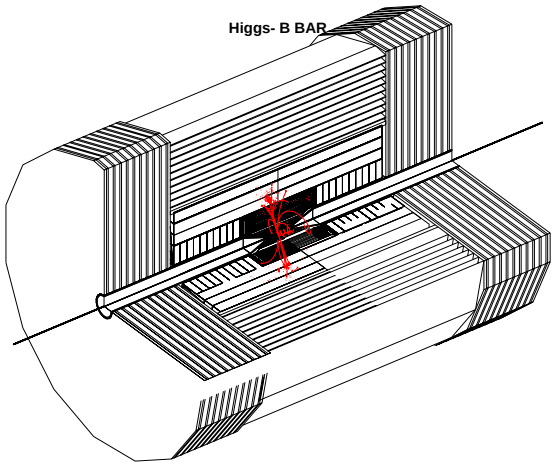

Figure 12 Cutaway of the strawman Geant detector with Higgs event superimposed. The 20 degree tungsten cone shields the interaction region from backgrounds.

10 Muon storage ring as neutrino factory

A major source of physics interest in the muon collider/storage ring idea has been the use of such rings to produce intense neutrino beams. The neutrinos are highly collimated with well defined flux and flavor content. For muon colliders with 1.5 TeV per beam, the neutrinos pose a radiation hazard in that as they emerge from the earth, the radiation from their interactions with matter will exceed the Federal limit, unless the collider is buried at depths exceeding 300 meters. The demands on cooling and bunch size are more relaxed for a storage ring than a collider. The collaboration currently plans to study the problems associated with a muon storage/ring neutrino factory as a first step towards a muon collider. There have been a string of papers exploring this option, beginning with[16]. Figure 13 and Figure 14 show the that the muon storage ring has the ability to extend the exclusion contours in the δm^2 ,$\sin^2(2\theta)$ plane by an order of magnitude. The plots shown in this case are for $\nu_{e\to\tau}$ oscillations, similar impressive limit gains can be obtained for other oscillation scenarios.

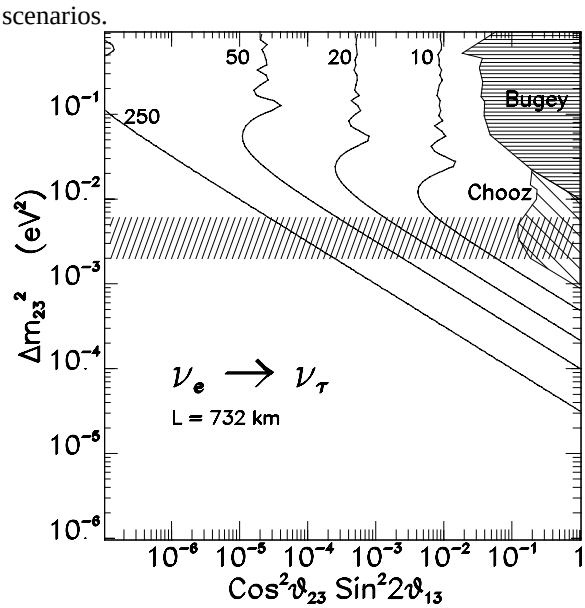

Figure 13 Single event contours for $\nu_{e\to\tau}$ oscillations for muon storage ring energies from 10-250 GeV. Baseline is from Fermilab to Soudan.

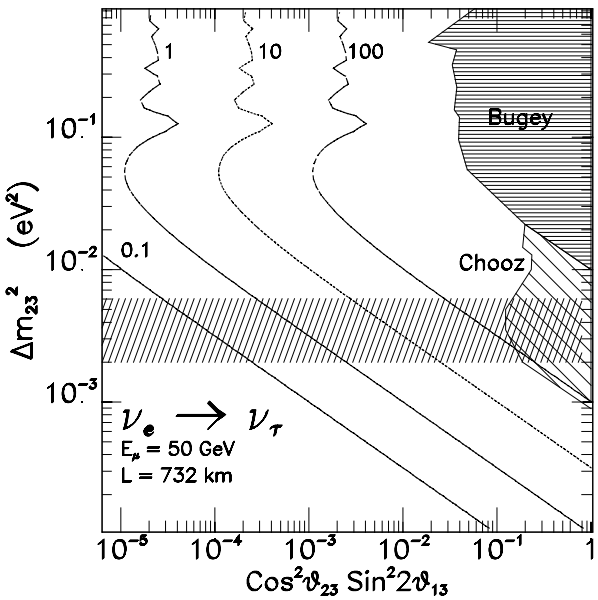

Figure 14 Event contours (0.1-100 events) for a 50 GeV storage ring for $\nu_{e\to\tau}$ oscillations

11 Conclusions

The muon collider is a concept investigating further. Despite, or perhaps because of the horrendous challenges involved, it has managed to attract a large number of talented physicists to work on it. Not all the problems are solved, but impressive progress has been made on a number of fronts in recent years. The physics potential of a muon collider and its energy reach are impressive. Problems remain in beam optics, in cooling, acceleration and collision. Pattern recognition of events in the presence of the large backgrounds needs to be established on a firmer footing. Muon storage rings hold great promise as a means to extend greatly our understanding of the lepton sector and as a natural first step on the way to a muon collider.

12 References

[1] A storage ring for 10 BeV/c muons , J.Tinlot and D.Green, UR-875-76 (1965)

[2] G. I. Budker, Accelerators and Colliding Beams (in Russian), in Proc. 7 th Int. Conf. on High Energy Accel. (Yerevan, 1969), p. 33; extract: AIP Conf. Proc. 352, p.4 (1996).
[3] A.N Skrinsky, Intersecting Storage Rings at Novosibirsk, Proc. Int. Seminar on Prospects of High-Energy Physics (Morges, Mar. 1971), unpublished; extract: AIP Conf. Proc. 352, p. 6 (1996).
[4] D. Neuffer, Colliding Muons Beams at 90 GeV, Fermilab report FN-319 (July 1979);http://www-ppd.fnal.gov/muscan/munotes/mc-001.pdf
[5] D.Neuffer and R.Palmer , Progress towards a high energy high luminosity $\mu^+\mu^-$ collider,AIP conf Proc. 356 (1996) p.344.
[6] A.N. Skrinsky and V. V. Parkhomchuk, Methods of cooling beams of charged particles, Sov. J. Part. Nucl. 12, p. 223 (1981).
[7] S. Geer and R. Raja (eds.), Workshop on Physics at the First Muon Collider and at the Front End of the Muon Collider, (Fermilab, Nov. 1997), AIP Conf. Proc. 435 (1998) http://ppd.fnal.gov/conferences/femcpw97/plenary/talks.html
[8] Status of muon collider research and development and future plans, Charles M. Ankenbrandt, etal. (Muon Collider Collaboration)Phys. Rev. ST Accel. Beams 2,081001(1999)(73pages)
[9] Calibrating the energy of a 50x50 GeV Muon Collider, R.Raja, A. Tollestrup, Phys. Rev. D58, 013005(1998).
[10] A development plan for the Fermilab Proton Source, S.D.Holmes et al; Fermilab-TM-2021(1997).
[11] An R&D program for targetry at a muon collider, J. Alesi et. al, http://puhep1.princeton.edu/mumu/target/targetprop.ps
[12] V.Barger,M.Berger,J.Gunion and T.Han, Higgs boson physics in the s-channel at $\mu\mu$ colliders, Phys.Rep.286,1(1997)
[13] Narrow Technihadron production at the first muon collider, E.Eichten et.al, Phys.Rev.Lett.80,5489(1998).
[14] V.Barger,M.Berger,J.Gunion,T.Han,, Nucl Phys.B,51A,13(1996).
[15] I. Stumer, Private Communication. N. Mokhov private Communication.
[16] S.Geer, Phys Rev D 57,6989(1998).